J. Fluid Mech. (1981), *vol.* 109, *pp.* 217–237
Printed in Great Britain

A nonlinear electrohydrodynamic stability analysis of a thermally stabilized plane layer of dielectric liquid

By W. J. WORRAKER† AND A. T. RICHARDSON
Department of Engineering Mathematics, University of Bristol

(Received 18 July 1980)

The nonlinear stability of a thermally stabilized horizontal plane layer of dielectric liquid subjected to unipolar charge injection at a voltage near the linear instability threshold is investigated using a normal-mode cascade analysis valid for small perturbation amplitudes. In this first analysis, the primary mode is chosen to be a system of parallel rolls whose amplitude varies aperiodically with time. The branching behaviour at the critical voltage is found to reflect the distinction, apparent in the linear instability problem, between an essentially isothermal space-charge instability and an instability dominated by the effects of an ion mobility varying with temperature. The effect of motion on heat and charge transfer through the system is also considered. Furthermore, in certain cases it appears that overstability is the preferred form of linear instability.

1. Introduction

Perhaps the simplest configuration exhibiting the destabilizing effect of an electrical field on an otherwise thermally stable layer of dielectric liquid is the parallel plate system considered experimentally by Gross & Porter (1966) and Turnbull (1968*b*). Attempts to explain this phenomenon have been made by several authors including Turnbull (1968*a*), Roberts (1969), Takashima & Aldridge (1976), Bradley (1978) and, most recently, Worraker & Richardson (1979). This latter study has its motivation in the use of strong d.c. electric fields in the augmentation of single-phase heat transfer in non-polar dielectric liquids. In such a hostile environment local flow velocities and electric fields may be determined indirectly by means of laser doppler anemometry and the electro-optical Kerr effect respectively. However, temperature profiles are not easily obtainable. From a practical point of view therefore it is ultimately desirable to have a means of predicting changes arising from fluid motion in the more readily measurable system parameters such as heat flux and total electrical current. In order to achieve this, however, an analysis of nonlinear interactions is required.

The stationary linear instability analysis of a unipolar charge injection equilibrium in which the carrier mobility depends linearly on temperature has shown that two types of instability can be distinguished. Depending upon the amount of injected charge and the sign and magnitude of the temperature-induced variations in mobility across the layer, there appears either a thermally modified space-charge mode or a Bénard-type space-charge mode (Worraker & Richardson 1979). Although the destabilizing force is electrophoretic in both cases, in the former the instability is essentially

† Now at the Institute of Sound and Vibration Research, University of Southampton.

the same as in isothermal electroconvection (Felici 1969) whilst in the latter it is essentially due to the thermal variation of mobility. It might therefore be conjectured that if the equilibrium is subjected to aperiodic disturbances then the local nonlinear behaviour of the system should further reflect this distinction.

As a first step in the investigation of the nonlinear behaviour of the Worraker & Richardson model we employ a normal-mode cascade approach (Segel 1965). This weakly nonlinear method of analysis, involving a successive approximation procedure, was selected from among the various available techniques (Segel 1966; Joseph 1976) because of its close dependence on the linear problem and its relative simplicity of formulation. It is a local form of analysis whose validity is therefore restricted to small perturbation amplitudes. Implicit in the method is the idea that the energy of a flow disturbance is initially concentrated in a primary mode, usually the mode deemed most unstable by linear theory, which by self-interaction generates a secondary mode and by further interactions produces third- and higher-order modes. Whilst in principle this method may be extended to the case of an arbitrary number of primary modes we confine this first analysis to a system of parallel rolls characterized by a single horizontal wavenumber. Although we cannot determine the preferred planform of motion by this method, if the equilibrium is subcritically unstable against rolls we can, provided that turbulent motion does not occur, infer the likelihood of hysteretical phenomena. Furthermore we might in general expect the various physically possible planforms to lead to similar heat and charge transfer characteristics.

2. Formulation of the problem

2.1. *The equilibrium formulation*

The model investigated by Worraker & Richardson (1979) comprises a dielectric liquid contained between two perfectly conducting rigid horizontal planar electrodes of infinite extent. In a rectangular Cartesian co-ordinate system (x, y, z) the emitter is located in the plane $z = 0$ and the collector, which is maintained at earth potential, is located in the plane $z = d$. The liquid is assumed to be incompressible with constant kinematic viscosity ν, thermometric conductivity κ and electrical permittivity ϵ, and is subjected to autonomous unipolar charge injection. The carrier mobility K is assumed to vary linearly with temperature so that

$$K(T) = K_0[1 + k_1(T - T_0)], \tag{2.1}$$

where T denotes temperature, k_1 is a positive constant and the suffix '0', here and subsequently, indicates a quantity evaluated at the emitter. The governing electrohydrodynamic equations then possess a steady one-dimensional hydrostatic equilibrium solution in which electrical current density $\mathbf{j} = [0, 0, j(z)]$, electric field $\mathbf{E} = [0, 0, E(z)]$, space-charge density $Q = Q(z)$ and electrical potential $\phi = \phi(z)$. We find that

$$T = T_0 + \beta z, \quad K = K_0(1 + k_1 \beta z), \tag{2.2), (2.3}$$

$$j(z) = K(z)\, Q(z)\, E(z) = K_0 Q_0 E_0 = j_0, \tag{2.4}$$

$$E(z) = E_0 \left[1 + \frac{2Q_0}{\epsilon E_0} q(z)\right]^{\frac{1}{2}}, \quad Q(z) = \frac{K_0 Q_0}{K} \left[1 + \frac{2Q_0}{\epsilon E_0} q(z)\right]^{-\frac{1}{2}}, \tag{2.5), (2.6}$$

$$\phi(z) = \int_z^d E(z')\, dz', \tag{2.7}$$

where $q(z)$ is defined by

$$q(z) = K_0 \int_0^z \frac{dz'}{K(z')} = \begin{cases} \dfrac{1}{k_1\beta}\ln(1+k_1\beta z), & \beta \neq 0, \\ z, & \beta = 0, \end{cases} \tag{2.8}$$

and β denotes the average temperature gradient. The fixed temperature and potential boundary conditions

$$T(0) = T_0, \quad T(d) = T_0 + \beta d, \quad \phi(0) = \phi_0, \quad \phi(d) = 0 \tag{2.9}$$

are satisfied by this equilibrium provided that

$$E_0 \int_0^d \left[1 + \frac{2Q_0}{\epsilon E_0} q(z)\right]^{\frac{1}{2}} dz = \phi_0. \tag{2.10}$$

The fifth boundary condition required to specify the equilibrium fully is derived from an injection law. In essence we need only further specify the emitter space-charge density Q_0 as a function of E_0. In the limit of strong injection, i.e. space-charge-limited current, $Q_0 \to \infty$ in which case we specify the emitter field $E_0 = 0$ (cf. Richardson 1980).

2.2. *Perturbation equations*

When the equilibrium state (2.2)–(2.10) is perturbed the subsequent evolution of the system can be described in terms of a three-dimensional vector $\mathbf{X} = (\Omega, \Theta, \Phi)^T$, whose components Ω, Θ and Φ represent the non-dimensionalized perturbations in the z component of velocity, temperature and electrical potential respectively. The governing nonlinear partial differential equations can then be written in the form

$$\mathbf{L}(\mathbf{X}) = \mathbf{N}(\mathbf{X}), \tag{2.11}$$

where $\mathbf{L}$ and $\mathbf{N}$ denote real matrix differential operators. The linear matrix operator $\mathbf{L}$ is chosen to be independent of time and the voltage parameter λ, say, and only contains operators appropriate to the linear marginal-state problem. Incorporating the time derivatives explicitly in $\mathbf{L}$ would lead to a series of approximations that is not uniformly valid in time (cf. Segel 1965, 1966). On the other hand the nonlinear operator $\mathbf{N}$ contains time derivatives and 'out of balance' terms proportional to $\lambda - \lambda_c$, the deviation of the voltage parameter from its critical value as determined from the onset of linear instability.

By scaling lengths, velocity components, temperature and electrical potential against layer thickness d, κ/d, βd and ϕ_0 as well as K, Q and E against K_0, Q_0 and ϕ_0/d respectively and on writing

$$\nabla_1^2 = \nabla^2 - \frac{\partial^2}{\partial z^2},$$

$$R = \frac{\alpha_1 \beta g d^4}{\nu\kappa}, \quad P = \frac{\nu}{\kappa}, \quad M = \frac{1}{K_0}\left(\frac{\epsilon}{\rho_0}\right)^{\frac{1}{2}}, \quad B = \frac{P}{M^2},$$

$$\kappa_1 = k_1 \beta d, \quad C = \frac{Q_0 d^2}{\epsilon\phi_0}, \quad \lambda = \frac{\epsilon\phi_0}{\rho_0 \nu K_0}, \tag{2.12}$$

where α_1 is the liquid thermal expansion coefficient, we can define

$$\mathbf{L} \equiv \begin{bmatrix} 1 & -\nabla^2 & 0 \\ \nabla^4 & -R\nabla_1^2 & \lambda_c^2 l_{23} \\ CDQ & \lambda_c l_{32} & \lambda_c l_{33} \end{bmatrix}, \tag{2.13}$$

with
$$\left.\begin{aligned} l_{23}(\cdot) &= -B\nabla_1^2[E\nabla^2(\cdot) - C(DQ)(\cdot)], \\ l_{32}(\cdot) &= \kappa_1 BCE_0 D\left[\frac{(\cdot)}{K}\right], \\ l_{33}(\cdot) &= -B\left\{\frac{1}{E}D[KE^2\nabla^2(\cdot)] + C[D(KQ)]\,D(\cdot)\right\}. \end{aligned}\right\} \tag{2.14}$$

Here D denotes differentiation with respect to the non-dimensionalized z co-ordinate. Furthermore if we write $\mathbf{N}(\mathbf{X}) = [N_1(\mathbf{X}), N_2(\mathbf{X}), N_3(\mathbf{X})]^T$ then

$$N_1(\mathbf{X}) = -P\frac{\partial}{\partial t}\Theta - \mathbf{u}\,.\,\nabla\Theta, \tag{2.15}$$

$$\left.\begin{aligned} N_2(\mathbf{X}) = {} & \frac{\partial}{\partial t}(\nabla^2\Omega) - \frac{1}{P}\zeta_z + B(\lambda^2 - \lambda_c^2)\nabla_1^2[E\nabla^2\Phi - C(DQ)\,\Phi] \\ & + B\lambda^2\{\nabla^2\Phi D(\nabla^2\Phi) + \nabla\Phi\,.\,\nabla[D(\nabla^2\Phi)] - \nabla(D\Phi)\,.\,\nabla(\nabla^2\Phi) - (D\Phi)\,\nabla^4\Phi\}, \end{aligned}\right\} \tag{2.16}$$

$$\left.\begin{aligned} N_3(\mathbf{X}) = {} & P\frac{\partial}{\partial t}(\nabla^2\Phi) - \kappa_1 B(\lambda - \lambda_c)CE_0 D(\Theta/K) \\ & + B(\lambda - \lambda_c)\{E^{-1}D(KE^2\nabla^2\Phi) + C[D(KQ)]\,D\Phi\} \\ & + \mathbf{u}\,.\,\nabla(\nabla^2\Phi) + \kappa_1 B\lambda E^{-1}D(E^2\Theta\nabla^2\Phi) + \kappa_1 B\lambda C\nabla\Phi\,.\,\nabla(Q\Theta) \\ & - B\lambda[K(\nabla^2\Phi)(\nabla^2\Phi) + \nabla\Phi\,.\,\nabla(K\nabla^2\Phi)] \\ & - \kappa_1 B\lambda[\nabla\Phi\,.\,\nabla(\Theta\nabla^2\Phi) + \Theta(\nabla^2\Phi)(\nabla^2\Phi)], \end{aligned}\right\} \tag{2.17}$$

where $\mathbf{u}$ is the scaled fluid velocity vector, ζ_z is the z component of $\mathrm{curl}^2(\mathbf{u}\,.\,\nabla\mathbf{u})$ and the Boussinesq approximation for density variations has been made.

This ninth-order system of equations (2.11)–(2.17) is subject to the no-slip, fixed temperature, fixed potential and autonomous injection boundary conditions

$$\Omega = D\Omega = \Theta = \Phi = 0 \quad \text{at} \quad z = 0, 1, \tag{2.18}$$

and
$$D^2\Phi = 0 \quad \text{at} \quad z = 0. \tag{2.19}$$

In the space-charge-limited case, however, the autonomous injection condition (2.19) must be replaced by
$$D\Phi = 0 \quad \text{at} \quad z = 0. \tag{2.20}$$

2.3. *The iteration scheme*

The successive approximation employed here involves the expansion of the vector $\mathbf{X}$ and the right-hand side of (2.11) as power series in the time-dependent perturbation amplitude, $A(t)$, that satisfies an ordinary differential equation yet to be determined. We write
$$\mathbf{X} = A\mathbf{X}_0 + A^2\mathbf{X}_1 + A^3\mathbf{X}_2 + O(A^4) \tag{2.21}$$

and
$$\mathbf{N}(\mathbf{X}) = \mathbf{Y} = A^2\mathbf{Y}_1 + A^3\mathbf{Y}_2 + O(A^4), \tag{2.22}$$

where the $\mathbf{Y}_i$ $(i = 1, 2, 3, \ldots)$ are derived from the definitions (2.15)–(2.17). Equating coefficients of successive powers of A then gives rise to a sequence of equations of the form:
$$\mathbf{L}(\mathbf{X}_0) = 0; \tag{2.23a}$$
$$\mathbf{L}(\mathbf{X}_i) = \mathbf{Y}_i, \quad i = 1, 2, 3, \ldots . \tag{2.23b}$$

Equations (2.23a) together with the appropriate boundary conditions constitute just the linear instability problem whose solution provides eigenvalues, of which λ_c is the

lowest, and corresponding eigenmodes $\mathbf{X}_0$. In order to proceed further we must specify the (x, y) dependence or planform of the primary mode. As a first attempt we consider therefore two-dimensional parallel rolls characterized by a dimensionless wavenumber a so that

$$\mathbf{X}_0 = [\Omega_0(x,y,z),\ \Theta_0(x,y,z),\ \Phi_0(x,y,z)]^T = \boldsymbol{\chi}_0(z)\cos ax, \tag{2.24}$$

where

$$\boldsymbol{\chi}_0(z) = [V_0(z),\ G_0(z),\ F_0(z)]^T. \tag{2.25}$$

The ordinary differential equation satisfied by the amplitude $A(t)$ results from solvability criteria for the inhomogeneous differential equations (2.23*b*). Because of the unboundedness of the liquid layer and the special symmetry of the chosen primary planform, these criteria lead to a Landau-type equation which may be written in the form

$$dA/dt = \alpha s A - \gamma A^3, \tag{2.26}$$

correct to order A^5, where $s = (\lambda - \lambda_c)/\lambda_c$, and α and γ are taken to be order one quantities implying that $dA/dt \sim A^3$, and $s \sim A^2$. Since (2.26) is only relevant for $|s| \ll 1$ and the definitions (2.15)–(2.17) contain terms proportional to

$$\lambda^2 - \lambda_c^2 = s(2+s)\lambda_c^2, \quad \lambda^2 = \lambda_c^2(1+s)^2 \quad \text{and} \quad \lambda = \lambda_c(1+s)$$

we make the leading-order approximations $\lambda^2 - \lambda_c^2 \simeq 2s\lambda_c^2$; $\lambda^2 \simeq \lambda_c^2$ and $\lambda \simeq \lambda_c$ for these expressions. Because of the rather special chosen form of $\mathbf{X}_0$ [cf. (2.24)] it appears that in solving $\mathbf{L}(\mathbf{X}_1) = \mathbf{Y}_1$ we do not require a solvability condition. However, the solution does give rise to x-independent expressions for heat flux and current flow correct to order A^2. On the other hand, having of necessity constructed and solved the linear adjoint problem $\mathbf{L}^*(\mathbf{X}_0^*) = 0$, together with the adjoint boundary conditions, the solvability condition applied to the $\cos ax$ dependent part of the system $\mathbf{L}(\mathbf{X}_2) = \mathbf{Y}_2$ does produce an amplitude equation of the expected form (2.26).

3. The normal-mode cascade

3.1. *The second-order problem*

Since $\mathbf{Y}_1$ is composed of terms independent of x and terms proportional to $\cos 2ax$, we write the solution of the second-order problem $\mathbf{L}(\mathbf{X}_1) = \mathbf{Y}_1$ in the form

$$\mathbf{X}_1 = \boldsymbol{\chi}_{10} + \boldsymbol{\chi}_{12}\cos 2ax, \tag{3.1}$$

so that the system of equations $\mathbf{L}(\mathbf{X}_1) = \mathbf{Y}_1$ may be decomposed into the two separate ordinary differential systems

$$\mathbf{L}^{(0)}\boldsymbol{\chi}_{10} = \mathbf{Y}_1^{(0)} \tag{3.2}$$

and

$$\mathbf{L}^{(2)}\boldsymbol{\chi}_{12} = \mathbf{Y}_1^{(2)}, \tag{3.3}$$

where $\boldsymbol{\chi}_{10} = (V_{10}, G_{10}, F_{10})^T$, $\boldsymbol{\chi}_{12} = (V_{12}, G_{12}, F_{12})^T$ and $\mathbf{L}^{(0)}$, $\mathbf{L}^{(2)}$ and $\mathbf{Y}_1^{(0)}$ and $\mathbf{Y}_1^{(2)}$ are defined in the appendix [cf. (A 1)–(A 7)]. The boundary conditions on $\boldsymbol{\chi}_{10}$ and $\boldsymbol{\chi}_{12}$ are the same as those on $\boldsymbol{\chi}_0$, in component form being

$$\left.\begin{aligned} &V_{10} = DV_{10} = G_{10} = F_{10} = 0 \quad \text{at} \quad z = 0, 1 \\ \text{and} \quad &D^2F_{10} = 0 \quad \text{at} \quad z = 0 \quad \text{(finite injection)} \\ \text{or} \quad &DF_{10} = 0 \quad \text{at} \quad z = 0 \quad \text{(SCLC)}, \end{aligned}\right\} \tag{3.4}$$

and similarly for the components of χ_{12}. It can be seen immediately from the definitions of $\mathbf{L}^{(0)}$ and $\mathbf{Y}_1^{(0)}$ that

$$D^4 V_{10} = 0, \tag{3.5}$$

which in conjunction with the above boundary conditions on V_{10} leads to

$$V_{10}(z) = 0. \tag{3.6}$$

This implies that there is no mean flow in the z direction to order A^2, and is a necessary consequence of the equation of continuity. We then find by integration and the application of boundary conditions on G_{10} that

$$G_{10}(z) = \frac{1}{2}\left[\int_0^z V_0(\xi)\, G_0(\xi)\, d\xi - z\int_0^1 V_0(\xi)\, G_0(\xi)\, d\xi\right]. \tag{3.7}$$

It is also possible to write down integral expressions for F_{10} in terms of G_{10}, V_0, G_0, F_0, K, E, Q and the dimensionless system parameters (2.12). The fact that only (3.2) is soluble by direct integration is related to the mean-field character of its solution, continuity and the constancy of mean heat flux and mean current flow across the layer. Having obtained numerical solutions to both (3.2) and (3.3), these latter two properties of the system may be used as a check on the solution of (3.2).

3.2. *Heat and charge transfer*

The heat flux in the z direction arises from both thermal diffusion and fluid convection. Spatial averaging over the horizontal (x, y) plane, denoted by a bar, leads to the dimensional expressions

$$\bar{H}_d = -k\partial\bar{T}/\partial z \tag{3.8}$$

and

$$\bar{H}_c = \rho c_p \overline{w(T-\bar{T})}, \tag{3.9}$$

for these respective contributions. The constant k is the liquid thermal conductivity, c_p its specific heat at constant pressure and w the z component of velocity. Since $\bar{T} = T_0 + \beta z + \overline{\delta T}$, in terms of the temperature perturbation δT, and by continuity $\bar{w} = 0$, the Nusselt number Nu, defined as the ratio of total averaged heat flux to the conductive heat flux in the absence of motion, may be expressed in the form

$$Nu = 1 + \frac{1}{\beta}\frac{\partial}{\partial z}\overline{\delta T} - \frac{1}{\beta\kappa}\overline{w\delta T}, \tag{3.10}$$

where $\kappa = k/\rho c_p$. In terms of dimensionless quantities this is equivalent to

$$Nu = 1 + D\overline{\Theta} - \overline{\Omega\Theta}, \tag{3.11}$$

which on substituting

$$\Omega = AV_0 \cos ax + A^2 V_{12} \cos 2ax + O(A^3) \tag{3.12}$$

and

$$\Theta = AG_0 \cos ax + A^2(G_{10} + G_{12}\cos 2ax) + O(A^3), \tag{3.13}$$

from (2.21), (2.24), (3.1) and (3.6) and using (3.7), reduces to

$$\begin{aligned} Nu &= 1 + A^2(DG_{10} - \tfrac{1}{2}V_0 G_0) + O(A^4) \\ &= 1 + A^2 DG_{10}(0) + O(A^4). \end{aligned} \tag{3.14}$$

From (3.14) we see that indeed the Nusselt number, as defined, is a system parameter independent of z.

The spatially-averaged z component of the current density, comprising terms due to drift and convection but neglecting charge diffusion, is given in dimensional variables by

$$\bar{j}_z = \overline{(Q-\epsilon\nabla^2\delta\phi)\left[(K+k_1K_0\delta T)\left(E-\frac{\partial\delta\phi}{\partial z}\right)+w\right]}, \tag{3.15}$$

where $\delta\phi$ is the perturbation in electrical potential. Then the electrical Nusselt number Ne, defined as the ratio of $\bar{j}_z$ to its value in the absence of motion, takes the dimensionless form

$$Ne = \frac{1}{CE_0}\overline{(CQ-\nabla^2\Phi)\left[(K+\kappa_1\Theta)(E-D\Phi)+\frac{\Omega}{B\lambda}\right]}. \tag{3.16}$$

Using (3.12) and (3.13) together with the expansion

$$\Phi = AF_0\cos ax + A^2(F_{10}+F_{12}\cos 2ax)+O(A^3) \tag{3.17}$$

then leads to

$$Ne = 1+\frac{A^2}{CE_0}\left\{-\tfrac{1}{2}[(D^2-a^2)F_0]\left(\kappa_1EG_0-KDF_0+\frac{V_0}{B\lambda_c}\right)\right.$$
$$\left.+(DE)[\kappa_1(EG_{10}-\tfrac{1}{2}G_0DF_0)-KDF_{10}]-KED^2F_{10}\right\}+O(A^3), \tag{3.18}$$

where again the approximation $\lambda \simeq \lambda_c$ has been made. It is a straightforward matter to show from the third equation of system (3.2) and the definitions (A 1) and (A 6) that the expression (3.18) is independent of z as expected. In the case of finite injection for which $D^2F_{10}(0) = 0$ [cf. (3.4)] we find that evaluating Ne at the emitter gives

$$Ne = 1-\frac{A^2DF_{10}(0)}{E_0}+O(A^4). \tag{3.19}$$

However, in the case of space-charge-limited current a filtering of the singular behaviour of D^2F_0 and of D^2F_{10} is necessary if the expression (3.18) is to be evaluated at $z = 0$.

In general both Nu and Ne as given by (3.14) and (3.18) are functions of time and of the scaled voltage parameter s. Their explicit dependence on these quantities, however, can only be determined by evaluating constants α and γ and then solving the amplitude equation (2.26).

3.3. *The amplitude equation*

The solvability condition required to guarantee the existence of a non-trivial solution of the third-order problem

$$\mathbf{L}(\mathbf{X}_2) = \mathbf{Y}_2 \tag{3.20}$$

is derived from the theory of the Fredholm alternative (see, for example, Ince 1927; Milne 1980). In the present context this implies that $\mathbf{Y}_2$ must be orthogonal to the null space of the adjoint operator $\mathbf{L}^*$. Then the amplitude equation is derived from the constraint

$$\langle \mathbf{Y}_2, \mathbf{X}_0^* \rangle = 0, \tag{3.21}$$

where $\mathbf{X}_0^*$ is any solution of the linear adjoint problem

$$\mathbf{L}^*(\mathbf{X}_0^*) = 0, \tag{3.22}$$

and where the inner product may be defined by

$$\langle \mathbf{f}, \mathbf{g} \rangle = \int_0^1 \left[\int_0^{\pi/a} \mathbf{f}(x,z) \cdot \mathbf{g}(x,z)\, dx \right] dz \tag{3.23}$$

for any square integrable vector functions $\mathbf{f}$ and $\mathbf{g}$. The adjoint operator $\mathbf{L}^*$ and the adjoint boundary conditions are derived from the definition

$$\langle \mathbf{L}(\mathbf{f}), \mathbf{g} \rangle = \langle \mathbf{f}, \mathbf{L}^*(\mathbf{g}) \rangle. \tag{3.24}$$

Performing these integrations we find that

$$\mathbf{L}^* \equiv \begin{bmatrix} 1 & \nabla^4 & CDQ \\ -\nabla^2 & -R\nabla_1^2 & \lambda_c l_{23}^* \\ 0 & \lambda_c l_{32}^* & l_{33}^* \end{bmatrix}, \tag{3.25}$$

where

$$\left.\begin{aligned} l_{23}^*(\cdot) &= \frac{-\kappa_1 BCE_0}{K} D(\cdot), \\ l_{32}^*(\cdot) &= -B\lambda_c \nabla_1^2 \{\nabla^2[E(\cdot)] - C(DQ)(\cdot)\}, \\ l_{33}^*(\cdot) &= B\lambda_c \nabla^2 \left[KE^2 D\left(\frac{\cdot}{E}\right) \right] + B\lambda_c CD\{[D(KQ)](\cdot)\}. \end{aligned}\right\} \tag{3.26}$$

Furthermore, on writing

$$\mathbf{X}_0^* = \boldsymbol{\chi}_0^*(z) \cos ax = [V_0^*(z), G_0^*(z), F_0^*(z)]^T, \tag{3.27}$$

the adjoint boundary conditions are found to be

$$\left.\begin{aligned} V_0^* = G_0^* = DG_0^* = 0 \quad &\text{at} \quad z = 0, 1, \\ F_0^* = DF_0^* = 0 \quad &\text{at} \quad z = 1 \end{aligned}\right\} \tag{3.28}$$

and

$$E_0 DF_0^* - CF_0^* = 0 \quad \text{at} \quad z = 0 \quad \text{(finite injection)},$$

or

$$F_0^* = 0 \quad \text{at} \quad z = 0 \quad \text{(SCLC)}. \tag{3.29}$$

Once the adjoint problem (3.22) has been solved and the integrations implied by (3.21) performed we can obtain the Landau amplitude equation (2.26) with constants α and γ given by

$$\alpha = -\frac{(I_{22} + I_{32})}{(I_{11} + I_{21} + I_{31})}, \quad \gamma = \frac{(I_{13} + I_{23} + I_{33})}{(I_{11} + I_{21} + I_{31})}, \tag{3.30}$$

where the various integrals I_{ij} are defined implicitly in the appendix [cf. (A 8)–(A 19)]. It is clear that these values of α and γ then determine the character of the branching steady solutions of amplitude A_e, given by

$$A_e = \pm (\alpha s/\gamma)^{\frac{1}{2}}, \tag{3.31}$$

in the immediate vicinity of the bifurcation point.

4. Numerical analysis

4.1. *Numerical solution*

The systems of equations (2.23*a*), (3.22), (3.2) and (3.3) together with their respective boundary conditions were solved numerically, and the steady Nusselt numbers $Nu(A^2)$, $Ne(A^2)$ and parameters α and γ evaluated on a CDC 7600 machine using an integrated Chebyshev collocation program based on that used to solve the linear

problem (Worraker & Richardson 1979).† The case of space-charge-limited current was solved separately because of the necessity of filtering out the singular behaviour of the solution in the vicinity of the emitter. In all reported cases the degree of Chebyshev polynomial approximation was 25.

This integrated program involved first solving, in each case, the linear problem (2.23a) as before with $a = a_c$ corresponding to the minimum of the neutral stability curve $\lambda = \lambda(a)$. Slightly varying the value of wavenumber a had, as might have been expected, little effect on the nonlinear results in those cases investigated. Secondly the adjoint problem defined by (3.22), (3.25)–(3.29) was solved in a similar manner, and provided a useful check on the numerical method employed. Since the eigenvalues of these two problems must be complex conjugates of each other, the same real values of λ_c should be produced in both cases. It was found that the values of λ_c produced by solving these problems agreed to at least seven significant figures for $C \lesssim 2$, only to three or four figures for $C = 100$ and to four or five figures for the case of infinite C. The loss of close agreement probably reflects the progressively poorer convergence of the unfiltered Chebyshev series found as C increases beyond the $O(1)$ range. A further point of note is that the normalization of $\mathbf{X}_0$ and $\mathbf{X}_0^*$ was achieved by taking $V_0(\frac{1}{2})$ and $G_0^*(\frac{1}{2})$ respectively as unity. A possible alternative would have been to use $\max|V_0(z)|$ and $\max|G_0^*(z)|$ for $z \in [0, 1]$ but this produced very similar magnitudes for V_0, G_0^* etc. and indeed gave identical results for $Nu(s)$ and $Ne(s)$.

Solution of the second-order mean-field problem (3.2) was by a Chebyshev collocation technique so that it was transformed into the linear algebraic form

$$\mathbf{L}_{10}\mathbf{x}_{10} = \mathbf{y}_{10}, \tag{4.1}$$

where $\mathbf{x}_{10}$ and $\mathbf{y}_{10}$ are $3N+3$ element column vectors and $\mathbf{L}_{10}$ is a $(3N+3)\times(3N+3)$ matrix, N being the degree of Chebyshev polynomial representation of $\boldsymbol{\chi}_0$, $\boldsymbol{\chi}_0^*$, $\boldsymbol{\chi}_{10}$ and $\boldsymbol{\chi}_{12}$. Matrix $\mathbf{L}_{10}$ consists of nine $(N+1)\times(N+1)$ blocks corresponding to the nine operators constituting the elements of $\mathbf{L}^{(0)}$ together with the appropriate boundary-equation operators. The particular choice of collocation points and the location of boundary conditions corresponded to those used in the numerical linear problem [cf. Worraker & Richardson 1979].

The quantities $r_1 = \lim_{A\to 0}[(Nu-1)/A^2]$ and $r_2 = \lim_{A\to 0}[(Ne-1)/A^2]$, as defined by using the first equation (3.14) and (3.18) respectively, were evaluated for various $z \in [0, 1]$ by reconstructing the components of $\boldsymbol{\chi}_0(z)$ and $\boldsymbol{\chi}_{10}(z)$ using the appropriate Chebyshev coefficients. In addition to providing values therefore for $dNu/d(A^2)$ and $dNe/d(A^2)$ at the point of bifurcation, this exercise provided a check on the consistency of the results of the mean field problem. As a further check the coefficients of A^2 in the second line of (3.14) and (3.19) were also calculated. These checks were found to give mutually consistent results to at least seven significant figures for both r_1 and r_2 whenever $C \leqslant 2$. Indeed the worst variation in r_1 for any value of C was in the fifth significant figure. However, r_2 was found to vary significantly with z, by at most a factor of two, for finite but large ($\simeq 100$) values of C. This was again attributed to the poor Chebyshev polynomial representation of the unfiltered functions $F_0(z)$ and $F_{10}(z)$.

The fourth stage was the solution of the second-order problem (3.3) in a manner

† The definitions of M_1 and M_2 used in equation (4.4) in this reference are incorrect. They should read $M_1 = -(A_2 - B_2B_1^{-1}A_1)^{-1}C_2C_3^{-1}A_3$ and $M_2 = (A_2 - B_2B_1^{-1}A_1)^{-1}C_2C_3^{-1}B_3B_1^{-1}A_1$.

similar to that used for (3.2) with $\mathbf{L}^{(2)}, \boldsymbol{\chi}_{12}$ and $\mathbf{Y}_1^{(2)}$ replacing $\mathbf{L}^{(0)}, \boldsymbol{\chi}_{10}$ and $\mathbf{Y}_1^{(0)}$ respectively [cf. (4.1)]. The evaluation of α and γ was then accomplished by using standard integration routines, the integrand values being reconstructed directly from Chebyshev series representations.

4.2. *Numerical results*

A weakly stabilizing temperature difference of 1 °C across a layer of *n*-hexane or chlorobenzene of depth 0.5 mm or of 12 °C across a layer of transformer oil of depth 1 mm corresponds to a Rayleigh number $R \simeq -20$. For *n*-hexane we may estimate that $K_0 \simeq 10^{-7}\ \mathrm{m^2\,V^{-1}\,s^{-1}}$, $P \simeq 3{\cdot}8$, $M \simeq 1{\cdot}6$ and $B \simeq 1{\cdot}5$; for chlorobenzene $K_0 \simeq 4{\cdot}5 \times 10^{-8}\ \mathrm{m^2\,V^{-1}\,s^{-1}}$, $P \simeq 4{\cdot}6$, $M \simeq 4{\cdot}8$ and $B \simeq 0{\cdot}2$; and for transformer oil $K_0 \simeq 3 \times 10^{-10}\ \mathrm{m^2\,V^{-1}\,s^{-1}}$, $P \simeq 460$, $M \simeq 480$ and $B = 0{\cdot}002$. Most nonlinear results were obtained for the latter two fluids. Calculations were performed mainly for $R = -20$, $C = 10^{-3}, 10^{-2}, 10^{-1}, 1, 10, 100, \infty$ and $\kappa_1 = 0, 10^{-3}, 10^{-2}, 10^{-1}, 1$, the range of κ_1 values corresponding to the case of a cold emitter. Isothermal conditions were then modelled by setting $R = \kappa_1 = 0$.

We see from figures 1 and 2 that for $\kappa_1 \geqslant 0$ the (κ_1, C) plane may be divided into two main regions, according to the character of the bifurcating solutions as defined by the signs of α and γ. For large C and small κ_1, corresponding to the thermally modified space charge regime of the linear instability problem, we have a domain [cf. region (*a*)] of *unstable subcritical* solutions for which $\alpha > 0$ and $\gamma < 0$. For smaller C and larger κ_1, corresponding to the Bénard-type space-charge regime of the linear instability problem we have a domain [cf. region (*b*)] of *stable supercritical* solutions for which $\alpha > 0$ and $\gamma > 0$. We see also that the boundary between these two regions is shifted somewhat in the smaller C and larger κ_1 direction in going from $M \simeq 4{\cdot}8$ to $M \simeq 480$, and that for a fixed injection strength C it is again the value of $\kappa_1 B$ which appears to determine the dominant mode of instability.

On choosing an ion drift velocity scale $K_0\phi_0/d$, the slope $\alpha/\gamma\ [= (\alpha/\gamma)_{\mathrm{el}}]$ of the $A_{\mathrm{e}}^2(s)$ curve at $s = 0$ [cf. (3·31)] in region (*a*) appears generally to increase in magnitude with C and κ_1, taking values comparable to those of the related isothermal problem (Lacroix 1976). This is perhaps to be expected. On the other hand if region (*b*) is taken to correspond to a Bénard-type instability dominated by the effects of an ion mobility varying with temperature [cf. Worraker & Richardson 1979] we would expect the amplitude of steady convection to be controlled by the balance between convective heat flux and the lateral heat flux due to conduction. This suggests the use of a thermal velocity scale κ/d in this region. The resulting value s of $\alpha/\gamma\ [= (\alpha/\gamma)_{\mathrm{th}}]$ are found to be approximately constant ($\simeq 300$) for small C as suggested by our interpretation of the destabilising mechanism. In figure 2, corresponding to transformer oil, we find that for sufficiently strong injection a Bénard-type instability gives way to a space-charge-dominated one. From figure 1, on the other hand, corresponding to the case of chlorobenzene we see that the Bénard-type instability persists even for space-charge-limited currents whenever $\kappa_1 \gtrsim 0{\cdot}1$.

From a practical standpoint, perhaps the most interesting result of the heat flux calculation is the variation of Nusselt number with applied voltage. This is obtained from the product $r_1(\alpha/\gamma)_{\mathrm{th}}$ [see tables 1 and 2]. The parameter

$$r_1 = \lim_{A \to 0} [(Nu - 1)/A^2] \simeq 10^{-2}$$

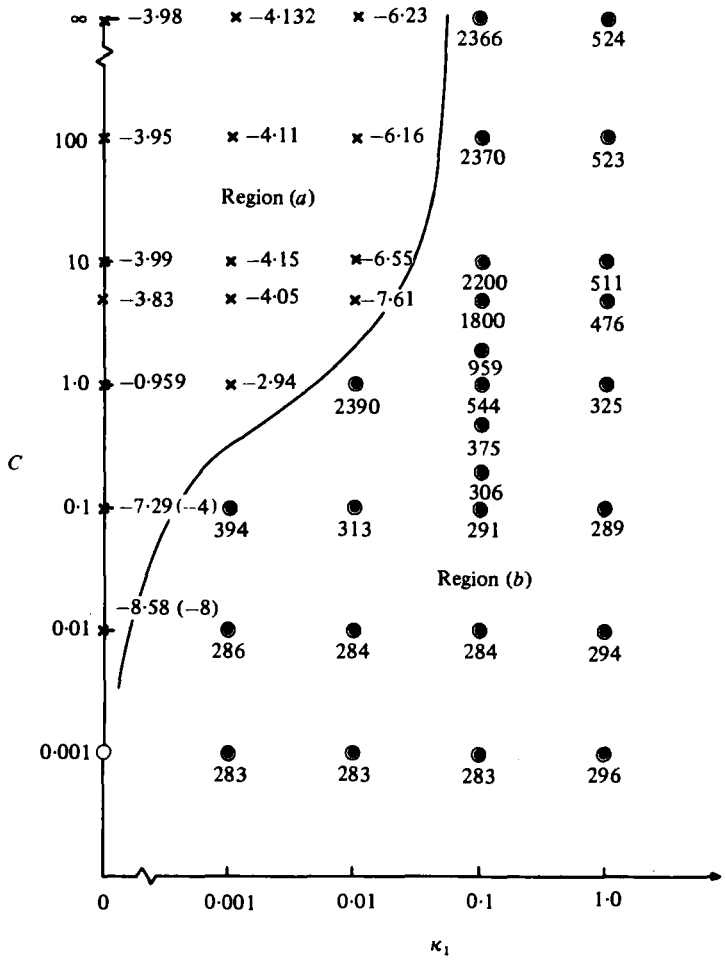

FIGURE 1. Nonlinear stability characteristics of a liquid with $B = 0{\cdot}2$, $P = 4{\cdot}6$ ($M \simeq 4{\cdot}8$) (e.g. chlorobenzene) and $R = -20$. The positive figures adjacent to data points are values of $(\alpha/\gamma)_{\text{th}}$. Negative figures are values of $(\alpha/\gamma)_{\text{el}}$. Region ($a$) is a domain of unstable subcritical solutions denoted by **x** and region (b) is a domain of stable supercritical solutions denoted by ●. The symbol ○ indicates that no solution was found.

in all cases and varies almost inversely with the wavenumber a. For most cases of supercritical bifurcation $r_1(\alpha/\gamma)_{\text{th}} \gtrsim 3$ implying that while steady roll motion prevails the Nusselt number will grow to several times unity before the voltage is raised to twice its critical value. This of course is only suggestive and presupposes that the analysis remains approximately valid outside the small $|s|$-range. The electrical Nusselt number is correspondingly obtained from the product $r_2(\alpha/\gamma)_{\text{el}}$ [see tables 1 and 2]. The parameter $r_2 = \lim_{A\to 0}[(Ne-1)/A^2] \simeq 0{\cdot}5B$ in region (b) of the (κ_1, C) plane whereas in region (a) it is an increasing function of C. For the case of supercritical bifurcation the electrical Nusselt number Ne is therefore proportional to $B(\alpha/\gamma)_{\text{el}}s$. Whilst the results for the subcritical bifurcation regime are not physically verifiable they do appear to be of the same order of magnitude as those found by Lacroix (1976).

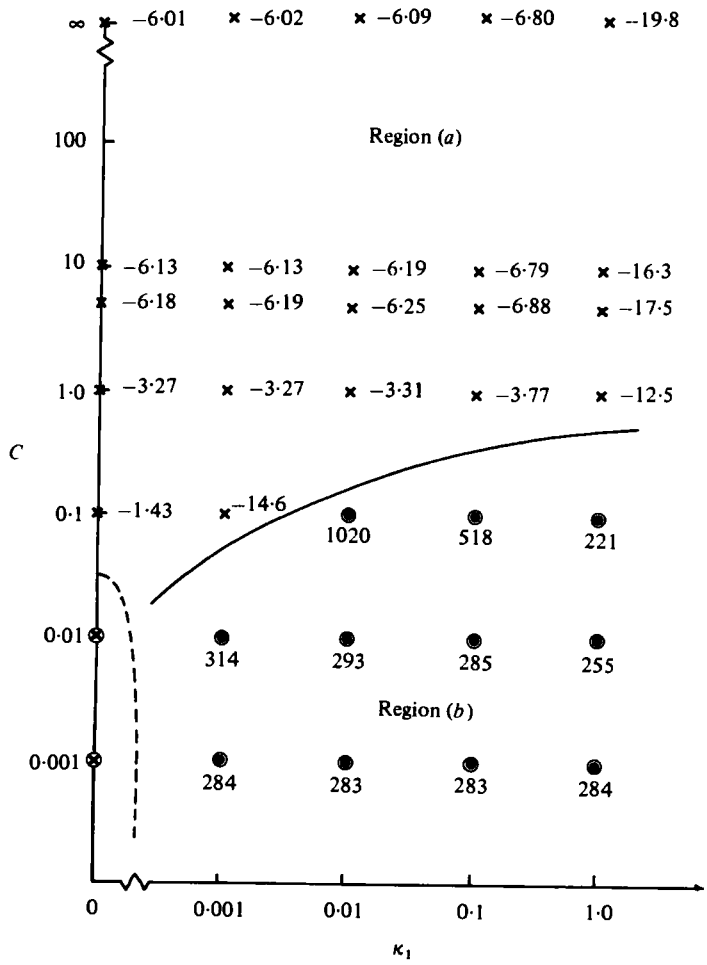

FIGURE 2. Nonlinear stability characteristics of a liquid with $B = 0{\cdot}002$, $P = 460$ ($M \simeq 480$) (e.g. transformer oil) and $R = -20$. The positive figures adjacent to data points are values of $(\alpha/\gamma)_{\text{th}}$. Negative figures are values of $(\alpha/\gamma)_{\text{el}}$. Region ($a$) is a domain of unstable subcritical solutions denoted by ✖ and region (b) is a domain of stable supercritical solutions denoted by ●. The symbol ⊗ denotes cases for which $\alpha < 0$.

A result worthy of special note is the occurrence of negative values of α for $\kappa_1 = 0$, $R = -20, B = 0{\cdot}002, P = 460$ when $C = 0{\cdot}001$ and $C = 0{\cdot}01$ [cf. figure 2]. This implies that the equilibrium configuration is linearly unstable to the steady mode under consideration when $\lambda < \lambda_c$ and linearly stable with respect to it when $\lambda > \lambda_c$. The reasons for these perhaps at first puzzling results were investigated numerically by considering the time dependent linear perturbation problem. A Chebyshev collocation technique was again used to determine eigenvalues corresponding to the growth rate $\sigma = \sigma_R + i\sigma_I$ and the associated complex eigenfunctions χ_0 for various values of λ in the vicinity of λ_c.

In the second case $C = 0{\cdot}01$ for example, for which $a = 4{\cdot}590$ and $\lambda_c = 2{\cdot}251117 \times 10^6$, as λ was increased through the range $2 \times 10^6 \leqslant \lambda \leqslant 4 \times 10^6$ all but two of the well-represented modes were found to be decaying with time ($\sigma_R < 0$), their decay rates

	a	C	λ_c	r_{1th}	r_{2el}	α/γ
$\kappa_1 = 0$	4·590	0·001	2·232906 (8)	7·15 (−3)	2·77 (−8)	—
	4·590	0·01	2·251117 (6)	7·15 (−3)	2·75 (−6)	−8·58 (−3)
	4·591	0·1	2·440227 (4)	7·11 (−3)	2·57 (−4)	−7·29 (−4)
	4·700	1·0	516·2250	6·73 (−3)	1·45 (−2)	−0·959
	5·066	5·0	177·33	6·05 (−3)	5·5 (−2)	−3·83
	5·138	10	166	5·93 (−3)	6 (−2)	−3·99
	5·164	100	162·2	5·89 (−3)	—	−3·95
	5·164	∞	162·20	5·89 (−3)	6·29 (−2)	−3·98
$\kappa_1 = 10^{-3}$	3·117	0·001	9·299741 (4)	1·02 (−2)	0·101	283
	3·131	0·01	2·934347 (4)	1·02 (−2)	0·101	286
	3·507	0·1	8060·134	9·19 (−3)	8·03 (−2)	394
	4·677	1·0	509·5479	6·77 (−3)	1·74 (−2)	−2·94
	5·063	5·0	177·1	6·05 (−3)	5·6 (−2)	−4·05
	5·135	10	165·4	5·93 (−3)	6 (−2)	−4·15
	5·162	100	162	5·89 (−3)	—	−4·11
	5·162	∞	162·0	5·89 (−3)	6·34 (−2)	−4·13
$\kappa_1 = 10^{-2}$	3·118	0·001	2·953241 (4)	1·02 (−2)	0·101	283
	3·125	0·01	9346·941	1·02 (−2)	0·102	284
	3·255	0·1	2896·402	9·83 (−3)	0·101	313
	4·514	1·0	461·5147	7·02 (−3)	3·79 (−2)	2390
	5·037	5·0	174·83	6·08 (−3)	6·1 (−2)	−7·60
	5·113	10	164	5·96 (−3)	7 (−2)	−6·55
	5·141	100	160·5	5·92 (−3)	—	−6·16
	5·141	∞	160·30	5·92 (−3)	6·8 (−2)	−6·23
$\kappa_1 = 0·1$	3·120	0·001	9742·552	1·02 (−2)	0·101	283
	3·130	0·01	3079·522	1·02 (−2)	0·102	284
	3·193	0·1	983·8425	1·00 (−2)	0·110	291
	3·274	0·2	699·8143	9·77 (−3)	0·114	306
	3·561	0·5	438·9790	9·00 (−3)	0·115	375
	3·988	1·0	298·3522	7·98 (−3)	0·107	544
	4·454	2·0	206·0811	7·03 (−3)	9·92 (−2)	959
	4·841	5·0	158·41	6·34 (−3)	0·103	1800
	4·945	10	151	6·17 (−3)	0·11	2200
	4·982	100	148·6	6·10 (−3)	—	2370
	4·982	∞	146·96	6·11 (−3)	0·10	2366
$\kappa_1 = 1·0$	3·129	0·001	4310·935	1·03 (−2)	9·20 (−2)	296
	3·144	0·01	1358·338	1·02 (−2)	9·49 (−2)	294
	3·201	0·1	432·8282	1·00 (−2)	0·107	289
	3·556	1·0	161·3287	9·01 (−3)	0·168	325
	4·330	5·0	121·58	7·13 (−3)	0·248	476
	4·493	10	120·7	6·79 (−3)	0·27	511
	4·560	100	121·1	6·65 (−3)	—	523
	4·561	∞	106·451	6·65 (−3)	0·2	524

TABLE 1. Numerical results of the nonlinear problem for the case $B = 0·2$, $P = 4·6$ (cf. chlorobenzene). Figures in brackets denote powers of ten. Positive values of α/γ correspond to a thermal velocity scale (suffix 'th') and negative values to an ion drift velocity scale (suffix 'el'). A horizontal bar denotes insufficient accuracy achieved.

	a	C	λ_c	r_{1th}	r_{2el}	α/γ
$\kappa_1 = 0$	4·590	0·001	2·232906 (8)	7·15 (−3)	2·77 (−8)	−9·97 (−8)†
	4·590	0·01	2·251117 (6)	7·15 (−3)	2·75 (−6)	−9·81 (−4)†
	4·591	0·1	2·440227 (4)	7·11 (−3)	2·57 (−4)	−1·43
	4·700	1·0	516·2250	6·73 (−3)	1·45 (−2)	−3·27
	5·066	5·0	177·33	6·05 (−3)	5·5 (−2)	−6·18
	5·138	10	166	5·93 (−3)	6 (−2)	−6·13
	5·164	∞	162·20	5·89 (−3)	6·29 (−2)	−6·01
$\kappa_1 = 10^{-3}$	3·125	0·001	9·268305 (5)	1·02 (−2)	1·02 (−3)	284
	3·259	0·01	2·765331 (5)	9·84 (−3)	9·48 (−4)	314
	4·500	0·1	2·295585 (4)	7·24 (−3)	3·46 (−4)	−14·6
	4·699	1·0	516·0318	6·74 (−3)	1·45 (−2)	−3·27
	5·066	5·0	177·34	6·05 (−3)	5·5 (−2)	−6·19
	5·138	10	165·6	5·93 (−3)	6 (−2)	−6·13
	5·164	∞	162·19	5·89 (−3)	6·28 (−2)	−6·02
$\kappa_1 = 10^{-2}$	3·131	0·001	2·936022 (5)	1·02 (−2)	1·03 (−3)	283
	3·198	0·01	9·036954 (4)	1·00 (−2)	1·05 (−3)	293
	4·125	0·1	1·647717 (4)	7·87 (−3)	7·47 (−4)	1020
	4·698	1·0	514·3385	6·74 (−3)	1·45 (−2)	−3·31
	5·066	5·0	177·4	6·05 (−3)	5·5 (−3)	−6·25
	5·138	10	166	5·93 (−3)	6 (−2)	−6·19
	5·164	∞	162·13	5·89 (−3)	6·24 (−2)	−6·09
$\kappa_1 = 0{\cdot}1$	3·155	0·001	9·589943 (4)	1·01 (−2)	1·06 (−3)	283
	3·249	0·01	2·915605 (4)	9·86 (−3)	1·19 (−3)	285
	3·785	0·1	7196·854	8·53 (−3)	1·51 (−3)	518
	4·683	1·0	501·1884	6·75 (−3)	1·42 (−2)	−3·77
	5·063	5·0	178·76	6·04 (−3)	5·2 (−2)	−6·88
	5·141	10	167	5·92 (−3)	6 (−2)	−6·79
	5·168	∞	161·61	5·87 (−3)	5·86 (−2)	−6·80
$\kappa_1 = 1{\cdot}0$	3·191	0·001	4·192408 (4)	1·01 (−2)	1·02 (−3)	284
	3·340	0·01	1·241914 (4)	9·63 (−3)	1·24 (−3)	255
	3·793	0·1	3180·806	8·46 (−3)	2·06 (−3)	221
	4·617	1·0	509·3583	6·76 (−3)	1·02 (−2)	−12·5
	5·036	5·0	204·90	6·02 (−3)	3·43 (−2)	−17·5
	5·191	10	190	5·78 (−3)	4 (−2)	−16·3
	5·228	∞	162·63	5·72 (−3)	3·14 (−2)	−19·8

TABLE 2. Numerical results of the nonlinear problem for the case $B = 0{\cdot}002$, $P = 460$ (cf. transformer oil). Figures in brackets denote powers of ten. Positive values of α/γ correspond to a thermal velocity scale (suffix 'th') and negative values to an ion drift velocity scale (suffix 'el'). Cases marked † correspond to negative values of α.

varying little with λ. On raising λ above 2×10^6 the decay rate of one of the two modes of interest decreases whilst that of the other increases. At $\lambda = \lambda_{c0}$ ($2{\cdot}175 \times 10^6 < \lambda_{c0} < 2{\cdot}2 \times 10^6$) these modes coalesce and subsequently become a complex conjugate pair of decaying oscillatory modes. At $\lambda = \lambda_{0s}$ ($2{\cdot}234 \times 10^6 < \lambda_{0s} < 2{\cdot}235 \times 10^6$) they become neutrally stable with $\sigma_R = 0$ and $|\sigma_I| \simeq 0{\cdot}11$ measured on a viscous time scale. Then at $\lambda = \lambda_s$ ($2{\cdot}2455 \times 10^6 < \lambda_s < 2{\cdot}246 \times 10^6$) these growing oscillatory (overstable) modes coalesce and form subsequently a pair of growing steady modes. As λ further increases beyond λ_s one steady mode increases its growth rate, but the other growth rate decreases, vanishing at $\lambda = \lambda_c = 2{\cdot}251117 \times 10^6$, so that the mode becomes a decaying one for $\lambda > \lambda_c$. This latter is clearly identifiable with the 'exchange

(*a*) *The case* $B = 0{\cdot}2, P = 4{\cdot}6$ (*cf. chlorobenzene*)

a	κ_1	λ_c	r_{1th}	r_{2st}	α/γ
5·164	0	162·20	5·89 (−3)	6·29 (−2)	−3·98
5·167	−0·001	162·4	5·89 (−3)	6·23 (−2)	−3·83
5·189	−0·01	164·21	5·86 (−3)	5·7 (−2)	−2·24
5·539	−0·1	190·41	5·47 (−3)	−1·6 (−2)	−0·466

(*b*) *The case* $B = 0{\cdot}002, P = 460$ (*cf. transformer oil*)

a	κ_1	λ_c	r_{1th}	r_{2st}	α/γ
5·164	0	162·20	5·89 (−3)	6·29 (−2)	−6·01
5·164	−0·01	162·27	5·89 (−3)	6·33 (−2)	−5·94
5·162	−0·1	162·95	5·90 (−3)	6·71 (−2)	−5·34
5·161	−0·2	163·8	5·91 (−3)	7·09 (−2)	−4·80
5·176	−0·4	164·52	5·89 (−3)	7·37 (−2)	−4·26

TABLE 3. Numerical results of the nonlinear SCLC problem in which $R = -20$ and $\kappa_1 \leqslant 0$.

of stabilities' mode studied in the nonlinear analysis. Significantly perhaps this analytical detour has revealed the existence of growing oscillatory modes at values of λ below λ_c. At the same time this study has confirmed both qualitatively and quantitatively the behaviour of the stationary modes deduced from their values of α: the value of $\sigma\,(=\sigma_R)$ as determined by the growth-rate analysis agreed well both in sign and in magnitude with the corresponding values of αs, for $|s| \ll 1$, deduced from the nonlinear problem. Further analysis has shown that the critical wavenumber for linear overstability in this case is 4·567.

Although it is not, in the present discussion, a specific aim to consider the case of a hot emitter, corresponding to $\kappa_1 < 0$, where for certain parameter values overstable oscillations of the kind just mentioned may be significant, we present in table 3 several results for the space-charge-limited current situation. It can be seen that the character of the instability found at $\kappa_1 = 0$ is retained in this limit of infinite C. However, in the case of chlorobenzene for the most negative $\kappa_1 B\,(= -0{\cdot}02)$ investigated, r_2 is found to be negative. This implies a reduction of the resulting charge transfer at the onset of motion.

Finally we consider the nonlinear isothermal problem for which $\kappa_1 = R = 0$ for various liquids characterized by differing values of M [cf. (2.12)]. The results are presented in figure 3 and table 4. It is immediately apparent that in all cases investigated the branching solutions exhibit unstable subcritical behaviour but that the degree of subcriticality depends strongly upon the value of M. For $M \simeq 4{\cdot}8$ we find that $|(\alpha/\gamma)_{el}|$ increases rapidly with C for $C \lesssim 1$. On the other hand for $M \simeq 480$ we find that $|(\alpha/\gamma)_{el}|$ increases slowly with C in a similar manner to that predicted by Lacroix (1976). In particular for $C = 0{\cdot}01$ we find that $(\alpha/\gamma)_{el} \simeq -1{\cdot}3$ and for $C = 10$ that $(\alpha/\gamma)_{el} \simeq -6{\cdot}1$ as compared with Lacroix's values of $-1{\cdot}6$ and $-4{\cdot}2$ respectively. We find that for $M^2C \lesssim 0{\cdot}25$, on rescaling α/γ in terms of a viscous velocity scale ν/d, that it takes a common value $\simeq -6{\cdot}5 \times 10^{+3}$ implying that the motion is controlled by viscosity, i.e. it is characterized by a Reynolds number.

In terms of an ion drift velocity scale the parameter r_2 is found to be independent of M as expected analytically, its qualitative behaviour as a function of C being again

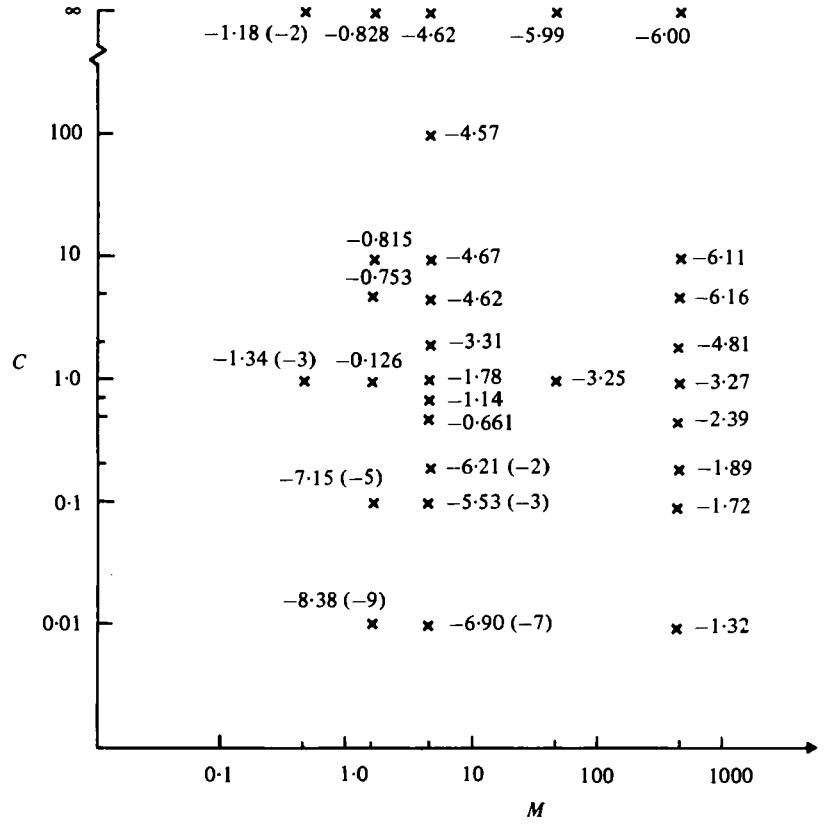

FIGURE 3. The effect of varying M in the nonlinear isothermal problem. The figures adjacent to data points are values of $(\alpha/\gamma)_{el}$, the solutions being unstable subcritical in all cases.

similar to that predicted by Lacroix using a mean-field analysis. The values obtained here, however, are smaller. For example for $C = \infty$ we find that $r_2 \simeq 0{\cdot}06$ whereas Lacroix finds $r_2 \simeq 0{\cdot}14$. On the other hand comparing values of $r_2(\alpha/\gamma)_{el}$ we find that the present results give for example $-0{\cdot}37$ for $C = 10$ in good agreement with the value of $-0{\cdot}38$ deduced from Atten & Lacroix (1979) who used a modal approximation technique with more than one horizontal mode.

5. Concluding remarks

It is clear from the results presented that the distinction between a thermally modified space-charge type of instability and a Bénard-type space-charge instability noted by Worraker & Richardson (1979) is further highlighted by a weakly nonlinear stability analysis. Once again the value of $\kappa_1 B$ is found to be important in determining which of these modes is dominant. The fact that we obtain a supercritical bifurcation for the Bénard-type mode and a subcritical bifurcation for the space-charge mode is in accordance with expectations based upon simple symmetric models of Bénard convection (Palm 1975) and isothermal unipolar electroconvection (Atten & Lacroix 1979).

	a	C	λ_c	r_{2cl}	$(\alpha/\gamma)_{cl}$
$M = 0{\cdot}48$	4·680	1·0	510·9926	1·45 (−2)	−1·34 (−3)
	5·138	∞	160·75	6·285 (−2)	−1·18 (−2)
$M = 1{\cdot}6$	4·571	0·01	2·227634 (6)	2·75 (−6)	−8·38 (−9)
	4·5725	0·1	2·414757 (4)	2·57 (−4)	−7·15 (−5)
	4·680	1·0	510·9926	1·45 (−2)	−0·126
	5·041	5·0	175·71	5·5 (−2)	−0·753
	5·113	10	164·1	6 (−2)	−0·815
	5·138	∞	160·75	6·285 (−2)	−0·828
$M = 4{\cdot}8$	4·571	0·01	2·227634 (6)	2·75 (−6)	−6·90 (−7)
	4·5725	0·1	2·414757 (4)	2·57 (−4)	−5·53 (−3)
	4·577	0·2	6595·051	9·59 (−4)	−6·21 (−2)
	4·607	0·5	1365·393	4·92 (−3)	−0·661
	4·634	0·7	821·9014	8·51 (−3)	−1·14
	4·680	1·0	510·9926	1·45 (−2)	−1·78
	4·827	2·0	258·5078	3·29 (−2)	−3·31
	5·041	5·0	175·71	5·5 (−2)	−4·62
	5·113	10	164·1	6 (−2)	−4·67
	5·128	100	160·8	—	−4·57
	5·138	∞	160·75	6·285 (−2)	−4·26
$M = 48$	4·680	1·0	510·9926	1·45 (−2)	−3·25
	5·138	∞	160·75	6·285 (−2)	−5·99
$M = 480$	4·571	0·01	2·227634 (6)	2·75 (−6)	−1·32
	4·5725	0·1	2·414757 (4)	2·57 (−4)	−1·72
	4·577	0·2	6595·051	9·59 (−4)	−1·89
	4·607	0·5	1365·393	4·92 (−3)	−2·39
	4·650	1·0	510·9926	1·45 (−2)	−3·27
	4·827	2·0	258·5078	3·29 (−2)	−4·81
	5·041	5·0	175·71	5·5 (−2)	−6·16
	5·113	10	164·1	6 (−2)	−6·11
	5·138	∞	160·75	6·285 (−2)	−6·00

TABLE 4. Numerical results for the nonlinear isothermal problem. Figures in brackets denote powers of ten. The horizontal bar denotes insufficient numerical accuracy achieved.

Although we have only investigated the case of small-amplitude roll motion near the onset of stationary linear instability, the results for Nusselt number Nu and electrical Nusselt number Ne together with the relevant values of α/γ provide clues as to the expected behaviour of a thermally stable layer of dielectric liquid subject to unipolar charge injection in the vicinity of the critical applied voltage. In the case of supercritical bifurcation, for both chlorobenzene and transformer oil, we find that the slope of the $Nu(s)$ curve at $s = 0$ is about 3 or greater. This implies a fairly rapid initial growth in the rate of heat transfer with voltage above critical. On the other hand the corresponding growth in the rate of charge transfer is at least an order of magnitude smaller. In the case of subcritical bifurcation a discontinuous transition to finite-amplitude motion is predicted. This in turn implies discontinuous changes in both heat flux and electrical current flow. Provided the flow remains laminar there will be associated hysteresis phenomena (Lacroix, Atten & Hopfinger 1975; Atten & Lacroix 1979).

A plausible mechanism for the occurrence of overstability when $\kappa_1 = 0$, R is small and negative and C is small in the electrical destabilization of Brunt–Väisälä

oscillations of the gravitationally stable fluid layer. With no electric field applied such oscillations are damped by viscosity, but viscous resistance may be overcome if sufficiently strong electrical body force fluctuations in phase with velocity can be induced. In the Felici 'hydraulic model' of electroconvection for $C \ll 1$ (Felici 1969), in the small amplitude limit, the net electrical driving force is directly proportional to velocity. It therefore appears that overstability of the kind envisaged may be excited provided that the oscillation is rapid enough not to be thwarted by thermal diffusion whilst at the same time being slow enough for space charge fluctuations to remain in phase with velocity. Hence we require that thermal diffusion time $\gg$ period of oscillation $\gg$ ion transit time, or equivalently that $B\lambda \gg (P|R|)^{\frac{1}{2}} \gg 1$. In order that such periodic motion be the preferred mode of instability we further require that the system be not yet unstable to aperiodic disturbances. Of the cases investigated in the nonlinear analysis those exhibiting negative values of α best satisfy these conditions for overstability. Typical values of $|\sigma_I|$ obtained from the growth rate calculations are of the same order of magnitude as the dimensionless Brunt–Väisälä frequency $(|R|/P)^{\frac{1}{2}}$. A preliminary numerical search in the $-0{\cdot}1 \leqslant \kappa_1 \leqslant 0$ domain, corresponding to a hot emitter, has suggested that overstability is indeed, in the case of small C, small B and small negative R, the preferred form of linear instability (cf. Turnbull 1968*a*, *b*). However, as C increases in magnitude the space-charge-controlled stationary instability becomes dominant. This may have important consequences in the field of electrohydrodynamic heat-transfer enhancement.

It is important to recognize the limitations inherent in this investigation. The normal-mode cascade analysis presented here is only applicable to small-amplitude motions when voltages are in the vicinity of critical for the onset of stationary linear instability. The local stability properties of branching solutions have only been considered for parallel rolls subject to disturbances of the same form, orientation and spatial periodicity. The range of validity of our results is further restricted by two important effects. The first is the transition to turbulent flow conveniently characterized by the Reynolds number of the velocity amplitude, for which a suitable critical value of 10 has been suggested (Lacroix *et al.* 1975). In the case of chlorobenzene calculations suggest that for a subcritical bifurcation the motion is probably turbulent from its onset whilst for supercritical bifurcation this transition is unlikely to occur until $\lambda \gtrsim 2\lambda_c$. On the other hand for transformer oil a subcritical bifurcation is likely to lead to a laminar flow except when $C \lesssim 0{\cdot}1$ and $\kappa_1 \lesssim 10^{-3}$, whereas for supercritical bifurcation the flow will remain laminar up to voltages well above λ_c. The second effect is the removal of charge from regions of the liquid moving towards the emitter when the velocity amplitude exceeds the ion drift velocity. The convective heat and charge transport laws may then be significantly modified. Imposing in the supercritical bifurcation case the restriction that velocity amplitude on an ion drift scale is unity, we find least upper bounds of $\simeq 1{\cdot}4\lambda_c$ for chlorobenzene and $\simeq 1{\cdot}2\lambda_c$ for transformer oil on the range of validity of our results.

Finally we have made the same modelling assumptions as Worraker & Richardson (1979) including that of the uniformity of charge injection at the emitter surface and the neglect of transient effects. Hexagonal convection cells may occur at the onset of motion in experiments performed under conditions similar to those of Atten & Lacroix (1979). The planform to be expected when the instability is dominated by the effect of varying mobility is still open to question. In addition finite container size, imperfect

thermal and electrical insulation properties of side walls and residual electrical conduction in the fluid will all affect system behaviour. In conclusion, these latter remarks remain conjectural until a programme of experimental work subject to adequate electrochemical control has been undertaken.

The above work was supported by a grant from the Science Research Council, grant number GR/A01131.

Appendix

The order A^2 system of nonlinear equations $\mathbf{L}(\mathbf{X}_1) = \mathbf{Y}_1$, may, using (3.1), be decomposed into the two separate systems (3.2) and (3.3). The operators $\mathbf{L}^{(0)}$, $\mathbf{L}^{(2)}$ are defined by

$$\mathbf{L}^{(0)} = \begin{bmatrix} 1 & -D^2 & 0 \\ D^4 & 0 & 0 \\ CDQ & \lambda_c l_{32} & \lambda_c l_{33}^{(0)} \end{bmatrix}, \tag{A 1}$$

where l_{32} is defined in (2.14) and

$$l_{33}^{(0)}(\cdot) = -BD\{KD[ED(\cdot)]\}, \tag{A 2}$$

and

$$\mathbf{L}^{(2)} = \begin{bmatrix} 1 & -(D^2-4a^2) & 0 \\ (D^2-4a^2)^2 & 4a^2R & \lambda_c^2 l_{23}^{(2)} \\ CDQ & \lambda_c l_{32} & \lambda_c l_{33}^{(2)} \end{bmatrix}, \tag{A 3}$$

where

$$l_{23}^{(2)}(\cdot) = 4a^2B[E(D^2-4a^2)(\cdot) - C(DQ)(\cdot)], \tag{A 4}$$

$$l_{33}^{(2)}(\cdot) = -B\left\{\frac{1}{E}D[KE^2(D^2-4a^2)(\cdot)] + C[D(KQ)]D(\cdot)\right\}. \tag{A 5}$$

On writing $\mathbf{Y}_1^{(0)} = [Y_{01}, Y_{02}, Y_{03}]^T$ and $\mathbf{Y}_1^{(2)} = [Y_{21}, Y_{22}, Y_{23}]^T$ we have

$$\left.\begin{aligned} Y_{01} &= -\tfrac{1}{2}D(V_0G_0), \quad Y_{02} = 0, \\ Y_{03} &= \tfrac{1}{2}D[V_0(D^2-a^2)F_0] + \tfrac{1}{2}\kappa_1 B\lambda_c D[EG_0(D^2-a^2)F_0 + (DE)G_0DF_0] \\ &\quad - \tfrac{1}{2}B\lambda_c D[K(DF_0)(D^2-a^2)F_0], \end{aligned}\right\} \tag{A 6}$$

and

$$\left.\begin{aligned} Y_{21} &= \tfrac{1}{2}(G_0DV_0 - V_0DG_0), \\ Y_{22} &= \frac{1}{P}[V_0D^3V_0 - (DV_0)D^2V_0] + a^2B\lambda_c^2[(DF_0)D^2F_0 - F_0D^3F_0], \\ Y_{23} &= \tfrac{1}{2}\{V_0D(D^2-a^2)F_0 - (DV_0)(D^2-a^2)F_0 \\ &\quad + \kappa_1 B\lambda_c\{D[G_0D(EDF_0)] - a^2[ED(G_0F_0) + 3(DE)G_0F_0]\} \\ &\quad - B\lambda_c\{D[K(DF_0)(D^2-a^2)F_0] - 2a^2KF_0(D^2-a^2)F_0\}\}. \end{aligned}\right\} \tag{A 7}$$

The definition of the integrals I_{11}, I_{21}, I_{31}, I_{22}, I_{32}, I_{13}, I_{23} and I_{33} is related to the $\cos ax$ component of the third-order problem $\mathbf{L}(\mathbf{X}_2) = \mathbf{Y}_2$ and the condition (3.21) which give

$$\langle Y_{11}V_0^* + Y_{12}G_0^* + Y_{13}F_0^* \rangle = 0, \tag{A 8}$$

where we have written $\mathbf{Y}_2^{(1)} = (Y_{11}, Y_{12}, Y_{13})^T$ and the inner product symbol $\langle \cdot \rangle$ now

only refers to the z-integration $\int_0^1 (\cdot)\,dz$. In this notation we may write

$$\langle Y_{11} V_0^* \rangle = \left\langle \left(\frac{dA}{dt} H_{11} + A^3 H_{13} \right) V_0^* \right\rangle = I_{11} \frac{dA}{dt} + I_{13} A^3, \tag{A 9}$$

$$\langle Y_{12} G_0^* \rangle = \left\langle \left(\frac{dA}{dt} H_{21} + sA H_{22} + A^3 H_{23} \right) G_0^* \right\rangle = I_{21} \frac{dA}{dt} + I_{22} sA + I_{23} A^3, \tag{A 10}$$

$$\langle Y_{13} F_0^* \rangle = \left\langle \left(\frac{dA}{dt} H_{31} + sA H_{32} + A^3 H_{33} \right) F_0^* \right\rangle = I_{31} \frac{dA}{dt} + I_{32} sA + I_{33} A^3, \tag{A 11}$$

and combining (A 8)–(A 11) we derive the amplitude equation (2.26). The individual H_{ij} have the following forms:

$$H_{11} = PG_0, \quad H_{21} = -(D^2 - a^2) V_0, \quad H_{31} = -P(D^2 - a^2) F_0, \tag{A 12), (A 13), (A 14}$$

$$H_{22} = 2[(D^2 - a^2)^2 V_0 + a^2 R G_0], \quad H_{32} = C(DQ) V_0, \tag{A 15), (A 16}$$

$$H_{13} = -\tfrac{1}{2}[V_0(2DG_{10} + DG_{12}) + 2G_{12} DV_0 + \tfrac{1}{2} G_0 DV_{12} + V_{12} DG_0], \tag{A 17}$$

$$\begin{aligned} H_{23} = {} & -\tfrac{1}{4} P^{-1}[2V_{12} D^3 V_0 + (DV_{12}) D^2 V_0 - 2(DV_0)(D^2 - 3a^2) V_{12} - V_0 D(D^2 - 3a^2) V_{12}] \\ & + \tfrac{1}{2} a^2 B \lambda_c^2 [2(DF_{10})(D^2 - a^2) F_0 - 2F_0 D^3 F_{10} + F_0 D(D^2 - 3a^2) F_{12} \\ & + 2(DF_0)(D^2 - 3a^2) F_{12} - (D^2 F_0) DF_{12} - 2(D^3 F_0) F_{12}], \end{aligned} \tag{A 18}$$

$$\begin{aligned} H_{33} = {} & \tfrac{1}{4}[4V_0 D^3 F_{10} + 4(DV_0)(D^2 - 4a^2) F_{12} + 2V_0 D(D^2 - 4a^2) F_{12} + (DV_{12})(D^2 - a^2) F_0 \\ & + 2V_{12} D(D^2 - a^2) F_0] \\ & + \tfrac{1}{2} \kappa_1 B \lambda_c \Big\{ \frac{1}{E} D[E^2 \{G_0 [2D^2 F_{10} + (D^2 - 4a^2) F_{12}] + (2G_{10} + G_{12})(D^2 - a^2) F_0\}] \\ & + C[(DF_0) D\{Q(2G_{10} + G_{12})\} + [D(2F_{10} + F_{12})] D(QG_0) + 2a^2 Q(F_0 G_{12} + G_0 F_{12})] \Big\} \\ & - \tfrac{1}{2} B \lambda_c \big\{ K\{2(DF_0) D^3 F_{10} + 4[(D^2 - a^2) F_0] D^2 F_{10} + 2[D(D^2 - a^2) F_0] DF_{10} \\ & + (DF_0) D(D^2 - 5a^2) F_{12} + 2(D^2 F_0)(D^2 - 3a^2) F_{12} + (D^3 F_0) DF_{12} - 2a^4 F_0 F_{12}\} \\ & + \kappa_1 [2(DF_0) D^2 F_{10} + (DF_0)(D^2 - 4a^2) F_{12} + (2F_{10} + F_{12})(D^2 - a^2) F_0] \big\} \\ & - \tfrac{1}{4} \kappa_1 B \lambda_c \big\{ 3D[G_0 (DF_0)(D^2 - a^2) F_0] - a^2 G_0 F_0 (D^2 - a^2) F_0 \big\}. \end{aligned} \tag{A 19}$$

Note that the particular forms given for H_{22} and H_{32} in (A 15) and (A 16) have been derived from component equations of (2.23a).

REFERENCES

Atten, P. & Lacroix, J. C. 1979 Nonlinear hydrodynamic stability of liquids subjected to unipolar injection. *J. Méc.* **18**, 469.

Bradley, R. 1978 Overstable electroconvective instabilities. *Quart. J. Mech. Appl. Math.* **31**, 381.

Felici, N. 1969 Phénomènes hydro et aérodynamiques dans la conduction des diélectriques fluides. *Rev. Gen. de l'Électricité* **78**, 717.

Gross, M. J. & Porter, J. E. 1966 Electrically induced convection in dielectric liquids. *Nature* **212**, 1343.

Ince, E. L. 1927 *Ordinary Differential Equations*. Longmans.

Joseph, D. D. 1976 *Stability of Fluid Motions I*, Tracts in Natural Philosophy, vol. 27. Springer.

LACROIX, J. C. 1976 Instabilités hydrodynamiques et électroconvection lors d'injection d'ions dans les liquides isolants isotropes, Thèse Doct. Sci. Phys., Université Scientifique et Medicale de Grenoble, France.

LACROIX, J. C., ATTEN, P. & HOPFINGER, E. J. 1975 Electroconvection in a dielectric liquid layer subjected to unipolar injection. *J. Fluid Mech.* **69**, 539.

MILNE, R. D. 1980 *Applied Functional Analysis*, p. 254. Pitman.

PALM, E. 1975 Nonlinear thermal convection. *Ann. Rev. Fluid Mech.* **7**, 39.

RICHARDSON, A. T. 1980 The linear instability of a dielectric liquid contained in a cylindrical annulus and subjected to unipolar charge injection. *Quart. J. Mech. Appl. Math.* **33**, 277.

ROBERTS, P. H. 1969 Electrohydrodynamic convection. *Quart. J. Mech. Appl. Math.* **22**, 211.

SEGEL, L. A. 1965 The structure of nonlinear cellular solutions to the Boussinesq equations. *J. Fluid Mech.* **21**, 345.

SEGEL, L. A. 1966 Nonlinear hydrodynamic stability theory and its applications to thermal convection and curved flows. In *Non-Equilibrium Thermodynamics, Variational Techniques and Stability* (ed. R. J. Donnelly, R. Herman & I. Prigogine), p. 165. University of Chicago Press.

TAKASHIMA, M. & ALDRIDGE, K. D. 1976 The stability of a horizontal layer of dielectric fluid under the simultaneous action of a vertical D.C. electric field and a vertical temperature gradient. *Quart. J. Mech. Appl. Math.* **29**, 71.

TURNBULL, R. J. 1968*a* Electroconvective instability with a stabilising temperature gradient. I. Theory. *Phys. Fluids* **11**, 2588.

TURNBULL, R. J. 1968*b* Electroconvective instability with a stabilising temperature gradient. II. Experimental results. *Phys. Fluids* **11**, 2597.

WORRAKER, W. J. & RICHARDSON, A. T. 1979 The effect of temperature-induced variations in charge carrier mobility on a stationary electrohydrodynamic instability. *J. Fluid Mech.* **93**, 29.